Available online at www.sciencedirect.com
SCIENCE DIRECT®
International Journal of Mass Spectrometry 228 (2003) 955–967
International Journal of Mass Spectrometry
www.elsevier.com/locate/ijms

Theoretical studies of methane elimination from $C_4H_9^+$ and H_2 elimination from $C_3H_7^+$

Charles E. Hudson, Sanju Eapen, David J. McAdoo*

Marine Biomedical Institute, University of Texas Medical Branch, 301 University Boulevard, Galveston, TX 77555-1043, USA

Received 3 December 2002; accepted 16 April 2003

Abstract

Experimental evidence indicates that CH_4 elimination from $C_4H_9^+$ forms $CH_3C^+{=}CH_2$, suggesting a 1,2-process. This reaction releases appreciable translational energy, and is formally Woodward–Hoffmann forbidden. However, according to its appearance energy it takes place at its thermochemical threshold. We investigated the reaction by theory because it might be an unprecedented concerted 1,2-alkane elimination. We found transition states for two pathways for CH_4 elimination from $C_4H_9^+$ isomers. The lower energy one involves migration of an H from a methyl to the central carbon of the *tert*-butyl cation followed by insertion of that H into a C–CH_3 bond to form $CH_3C^+{=}CH_2 + CH_4$; the other is a 1,1-elimination from protonated methylcyclopropane to produce $CH_2CHCH_2^+ + CH_4$. H_2 elimination from $C_3H_7^+$ was also characterized to determine how that reaction and CH_4 elimination from $C_4H_9^+$ may be related. In accord with earlier studies, we found H_2 elimination from $C_3H_7^+$ by a 1,1-elimination through a 1-propyl-like stage in which an H migrates from C1 to C2 to C3, joining an H from C3 in the latter part of the last step. Also in accord with previous studies, we found a 1,1-H_2 elimination from a protonated cyclopropane. The two pathways for H_2 elimination from $C_3H_7^+$ are quite similar to the corresponding two for CH_4 elimination from $C_4H_9^+$. One type of elimination involves H-migration from methyl to an adjacent positively charged site, further migration and insertion into a bond, and finally dissociation. The other pathway in both instances involves a 1,1-elimination from a pentavalent carbon in a protonated cyclopropane. These findings extend the scope of evidence that most formal 1,2-eliminations have transition states much like ones for 1,1-eliminations and add an alkane elimination to the 1,2-H_2 eliminations that essentially go through 1,1-transition states. CH_4 elimination from $C_4H_9^+$ also bypasses the Woodward–Hoffmann barrier that opposes a direct 1,2-elimination.

Keywords: $C_4H_9^+$; $C_3H_7^+$; Ab initio; Alkane elimination; Woodward–Hoffmann; Translational energy release; Concerted elimination; Ion–neutral complex

1. Introduction

Nearly all alkane eliminations from radical cations [1–7] and most from closed shell species [6,8–13] go through ion–neutral complexes in which the alkane is formed by H-transfer between the partners. There is only one known apparent concerted elimination of CH_4 from a cation, that from $CH_3CH{=}OH^+$ [14]. In that reaction the threshold for the simple bond cleavage for forming the $[^{\bullet}CH_3\ HCOH]^+$ complex is 195 kJ mol^{-1} above the transition state and 332 kJ mol^{-1} above the thermochemical threshold for

* Corresponding author. Tel.: +1-409-772-2939; fax: +1-409-762-9382.
E-mail address: djmcadoo@utmb.edu (D.J. McAdoo).

1387-3806/$ – see front matter © 2003 Elsevier Science B.V. All rights reserved.
doi:10.1016/S1387-3806(03)00238-0

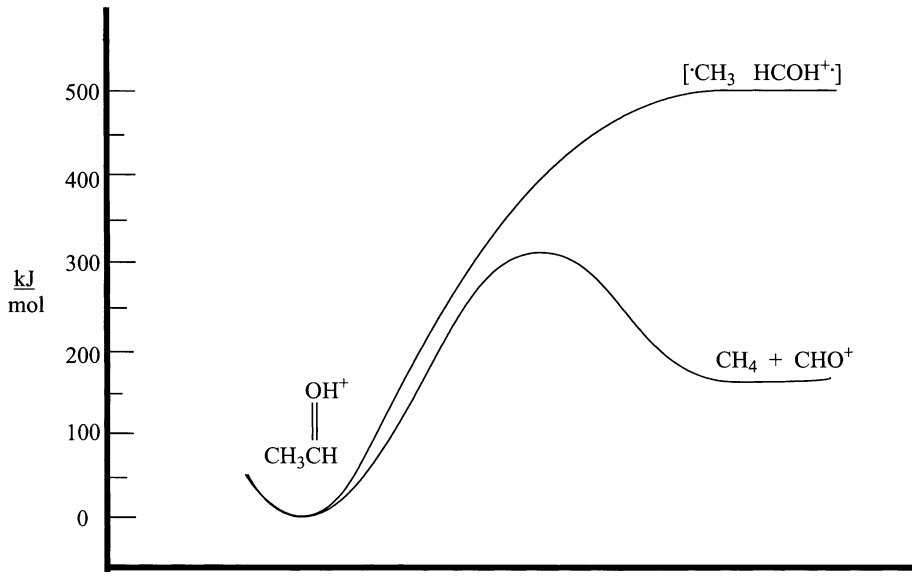

Fig. 1. Potential energy diagram for the elimination of CH_4 from $CH_3CH{=}OH^+$ taken from the results in Ref. [14].

$CH_4 + HCO^+$ formation [14] (Fig. 1). Thus, it is likely that alkane eliminations are concerted only when they can occur at energies below the threshold for forming the pertinent ion–neutral complex, i.e., below the threshold for the related simple bond cleavages.

The prominent CH_4 elimination from $C_4H_9^+$ to form $CH_3C^+{=}CH_2$ [15–19] could be of this type (Scheme 1), as the thermochemical threshold for dissociation to $^\bullet CH_3 + CH_3CH{=}CH_2{}^{\bullet+}$ is 211 kJ mol^{-1} higher than that for elimination of CH_4 to form $CH_3C^+{=}CH_2 + {}^\bullet CH_3$ [20]. A concerted alkane elimination would be of substantial interest because of the rarity of such reactions, a rarity attributable to 1,2-eliminations from closed shell species being Woodward–Hoffmann forbidden [21–23].

An appropriate and unique collisionally activated dissociation (CAD) spectrum of the $C_3H_5^+$ product provides strong evidence that $CH_3C^+{=}CH_2$ is formed upon CH_4 elimination from $C_4H_9^+$ [19,24]. This is a surprising product, given that the allyl cation is more stable than $CH_3C^+{=}CH_2$. The appearance energy measured for CH_4 elimination from *tert*-$C_4H_9^+$ is

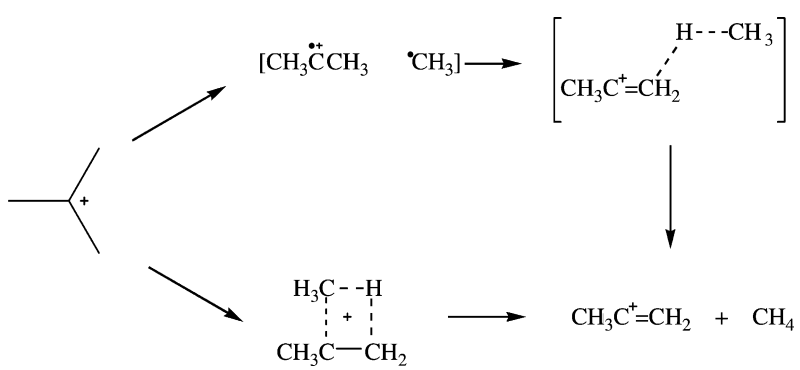

Scheme 1.

Table 1
Energies[a] obtained by theory for stationary points on the $C_4H_9^+$ potential surface

Structure	ZPE	B3LYP/6-31G*	QCISD/6-31G*	QCISD(T)/6-311G**
$(CH_3)_3C^+$	301.5	−157.554208 (0)	−156.996966 (0)	−157.134882 (0)
$CH_3CH^+CH_2CH_3$[b]	306.6	−157.532432 (62.3)	−156.974930 (63.0)	−157.114846 (57.7)
$CH_3CH^+CH_2CH_3$[c]	306.7		−156.972916 (68.3)	−157.114888 (57.8)
$CH_3CH^+CH_2CH_3$[d]	302.5	−157.531078 (61.7)	−156.9736532 (62.2)	−157.112785 (59.0)
$CH_3CH^+CH_2CH_3$[e]	302.2	−157.530831 (62.1)	−156.973611 (62.0)	−157.112261 (60.1)
PMCP[f]	310.4	−157.515326 (111.0)	−156.960957 (103.4)	−157.104159 (89.6)
TS(*iso*-Bu − CH_4)[g]	288.4	−157.474004 (197.5)	−156.911779 (210.6)	−157.056646 (192.3)
TS(PMCP − CH_4)[h]	294.5	−157.457049 (248.1)	−156.895366 (259.8)	−157.042743 (234.9)
$CH_3C^+{=}CH_2$	164.7	−116.955394	−116.56200	−116.648208
$CH_2CHCH_2^+$	176.9	−116.972219	−116.579154	−116.666123
CH_4	116.4	−40.518389	−40.353370	−40.405948
$CH_3C^+{=}CH_2 + CH_4$	281.1	−157.473783 (190.8)	−156.915374 (193.8)	−157.054156 (191.5)
$CH_2CHCH_2^+ + CH_4$	293.3	−157.490608 (158.8)	−156.932524 (161.0)	−157.072071 (156.7)
$CH_3CH{=}CH_2^{\bullet+}$	198.2	−117.564965	−117.157310	117.249422
$CH_3C^+CH_3$	192.4	−117.531886	−117.122741	
$^{\bullet}CH_3$	76.6	−39.842880	−39.689122	
$CH_3CH{=}CH_2^{\bullet+} + {}^{\bullet}CH_3$	274.8	−157.407845 (357.6)	−156.846432 (368.5)	−156.981723 (375.4)
$CH_3C^+CH_3 + {}^{\bullet}CH_3$	269.0	−157.374766 (438.6)	−156.811863 (453.5)	−156.948627 (456.5)

[a] Values in parentheses are in kJ mol^{-1} relative to $\Delta_f H$(*tert*-butyl = 0); they include ZPE corrections.
[b] For a 2-butyl ion with a C2C34C bond angle of 94.9° and a C1C2C3C4 dihedral angle of 92.0°.
[c] For a structure with a proton bridging C2 and C3; this structure was not found by B3LYP/6-31G* theory. The ZPE correction was therefore obtained using MP2-6-31G* theory.
[d] For a *trans* classical 2-butyl structure; the C1C2C3C4 dihedral angle is 154.8°.
[e] For a *cis* classical *sec*-butyl structure; the C1C2C3C4 dihedral angle is 5.9°.
[f] Protonated methylcyclopropane.
[g] From *tert*-$C_4H_9^+$ through *iso*-$C_4H_9^+$.
[h] For dissociation from protonated methylcyclopropane.

very near the thermochemical threshold for producing $CH_3C^+{=}CH_2 + CH_4$ (ca. 180 kJ mol^{-1}) [19], also consistent with the formation of $CH_3C^+{=}CH_2$. This low threshold might reflect a concerted elimination, as it is well below the energy required to form the $[CH_3C^+CH_3\ {}^{\bullet}CH_3]$ complex (ca. 456 kJ mol^{-1} based on the heats of formation of the separated products in Table 1). However, a concerted 1,2-elimination without a reverse barrier would contrast with properties of known 1,2-H_2 eliminations [25]. Although a theoretical characterization of much of the $C_4H_9^+$ potential surface exists [26], CH_4 elimination from $C_4H_9^+$ has not been described by theory. Therefore, in light of the potentially unusual nature of this reaction, we undertook its characterization by theory. We also investigated the analogous reaction, H_2 elimination from $C_3H_7^+$, to see whether pathways for H_2 and CH_4 eliminations are closely related. These studies are particularly appropriate to this volume because Professor Schwarz characterized the elimination of H_2 from *c*-$C_3H_7^+$ by theory many years ago [27].

2. Stationary points

We sought pathways for CH_4 elimination from $C_4H_9^+$ and H_2 from $C_3H_7^+$ utilizing hybrid functional and ab initio theory [28]. Table 1 gives the energies obtained for relevant $C_4H_9^+$ isomers, their dissociation products, and transition states that we located for CH_4 elimination. Corrections for zero point energy (ZPE) contributions were made using B3LYP/6-31G* frequencies together with scaling factors established by Scott and Radom [29]. Transition states were identified based on the presence of one

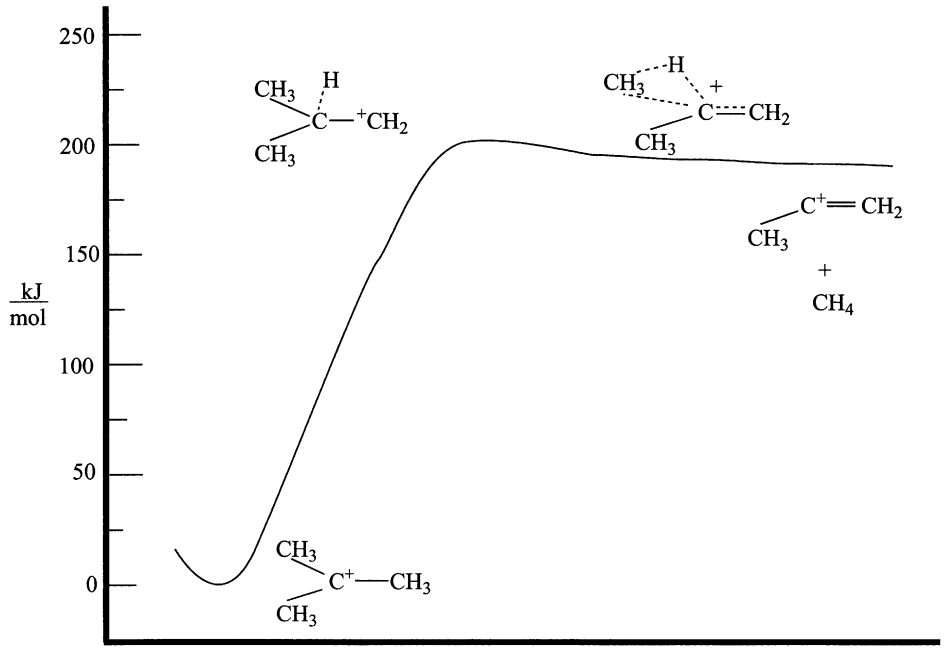

Fig. 2. Potential energy diagram for methane elimination from $C_4H_9^+$ through an isobutyl-like stage based on energies obtained by QCISD(T)/6-311G**//QCISD/6-31G* + ZPE theory.

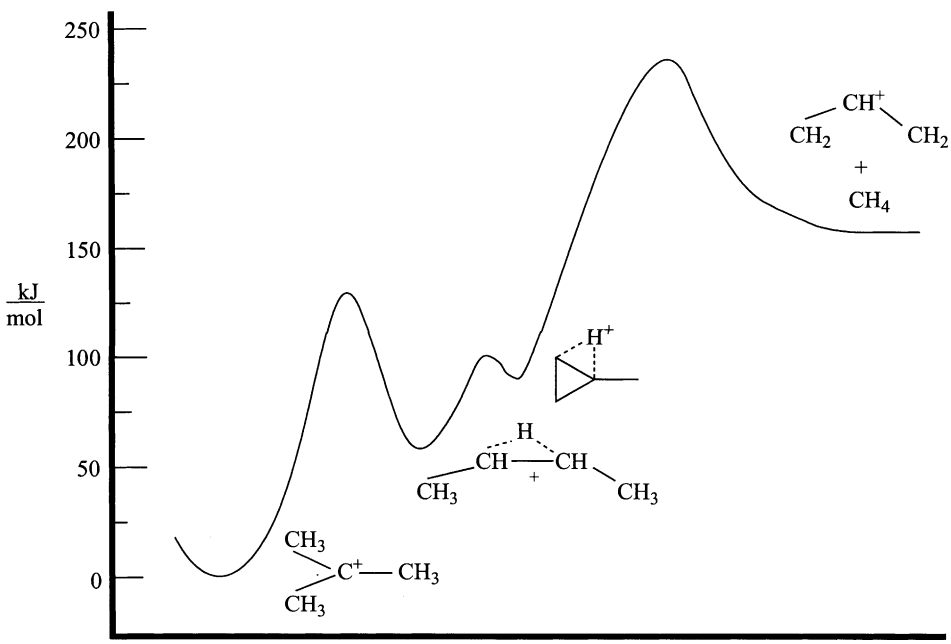

Fig. 3. Potential energy diagram for methane elimination from $C_4H_9^+$ through protonated methylcyclopropane based on energies obtained by QCISD(T)/6-311G**//QCISD/6-31G* theory.

negative eigenvalue in their force constant matrices. Potential energy diagrams for the CH_4 elimination pathways from $C_4H_9^+$ based on energies obtained by theory are given in Figs. 2 and 3. Figs. 4–9 give many of the optimized structures obtained by QCISD/6-31G* theory for the pertinent energy minima: the *tert*-butyl cation, two 2-butyl structures, protonated methylcyclopropane, and transition states for CH_4 elimination from $C_4H_9^+$. Throughout this work, atoms in $C_4H_9^+$ isomers are specified according to the labeling in the following diagrams (1–3).

Diagram 1

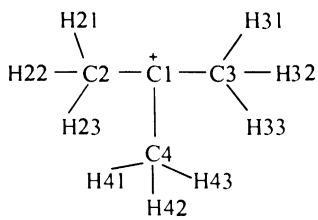

Diagram 2

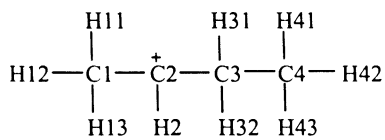

Diagram 3

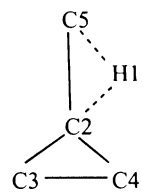

Our *tert*-$C_4H_9^+$ structure contained three almost but not quite identical methyls with no unusual features (Fig. 4). Four stable 2-butyl isomers were characterized, all in the energy range 57.7–59.2 kJ mol^{-1} above *tert*-$C_4H_9^+$. Two of these structures are given in Figs. 5 and 6. The most stable of these resembles a classical structure, but has a C2C3C4 bond angle of 94.9°, as compared to a corresponding angle of 119.6° in the classical *cis* structure. It also has a C1C2C3C4 dihedral angle close to 90° (Fig. 5). The *trans* C2–C3 proton-bridged form was only 0.1 kJ mol^{-1} higher than the most stable secondary structure in energy. The classical *cis* (Fig. 6) and *trans* isomers were slightly higher in energy than the bridged form. In a previous study, five 2-butyl isomers were found in the energy interval 56–66 kJ mol^{-1} above *tert*-$C_4H_9^+$, an energy range that encompasses ours for those structures. In the earlier study, the H-bridged structure with C2 symmetry was the most stable species. In contrast to that study [26], we characterized only the *trans*-bridged structure. Earlier investigators also included among *sec*-butyl structures one resembling methylated propene or a corner-protonated methylcyclopropane, a structure resembling ours with the 94.9° C2C3C4 angle. Although there are some small differences in energies, our results for the 2-butyl conformers are in very good agreement with those obtained previously. Our structure for protonated methylcyclopropane (Fig. 7) was also similar to the one found earlier. For that ion, the C2–C5, C2–H1, and C3–C4 distances varied only by 0.0–0.008 Å between the two studies, despite the use of different levels of theory. However, our C2–C3 distance was 0.162 Å less and our C2–C4 and C4–H1 distances were respectively 0.05 and 0.107 Å greater than theirs. Agreement of energies between the two studies was quite satisfactory, 90 kJ mol^{-1} vs. 92 kJ mol^{-1}.

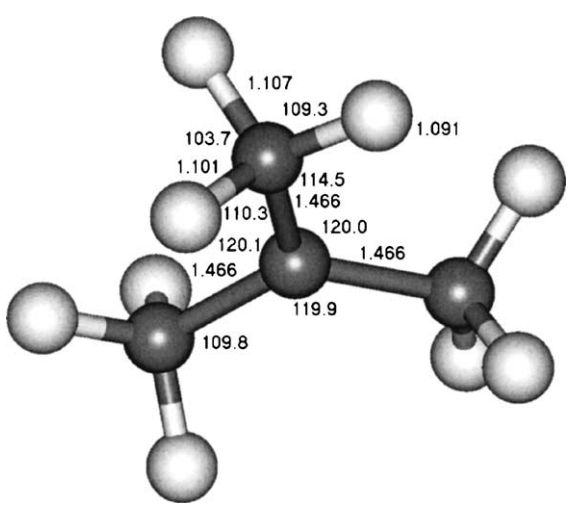

Fig. 4. Optimized structure for the *tert*-butyl ion obtained by QCISD/6-31G* theory.

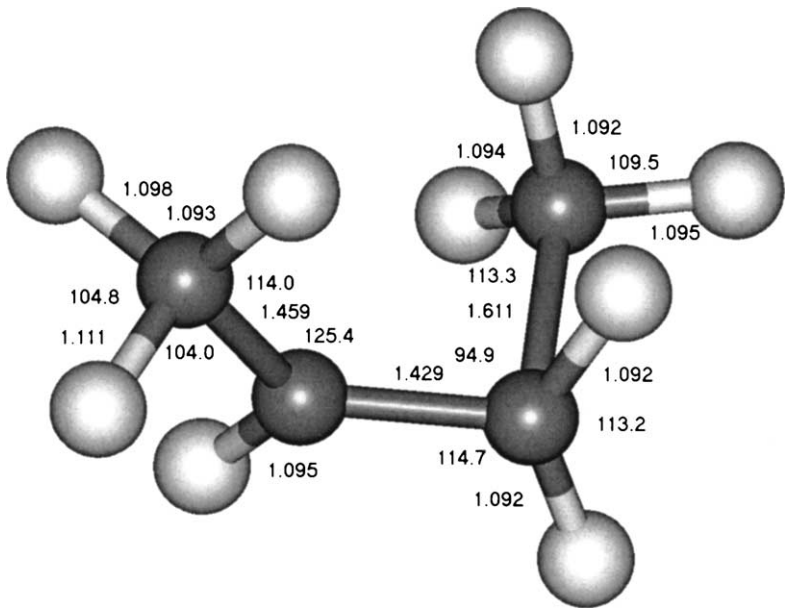

Fig. 5. Optimized structure for a 2-butyl ion with the CCC angle bent to 94.9°, obtained by QCISD/6-31G* theory.

3. Methane elimination from $C_4H_9^+$

We found two pathways for CH_4 elimination from $C_4H_9^+$, one through an isobutyl-like stage (potential energy surface in Fig. 2), and one through a corner-protonated methylcyclopropane (potential energy surface in Fig. 3). In the first, a hydrogen migrates from a methyl past C1 to insert into the C1–C3 bond to form the eliminated CH_4 and $CH_3C^+{=}CH_2$. The second pathway goes through protonated methylcyclopropane to the allyl ion.

According to our highest level of theory, formation of $CH_3C^+{=}CH_2$ by CH_4 elimination takes place without a reverse barrier, in agreement with the

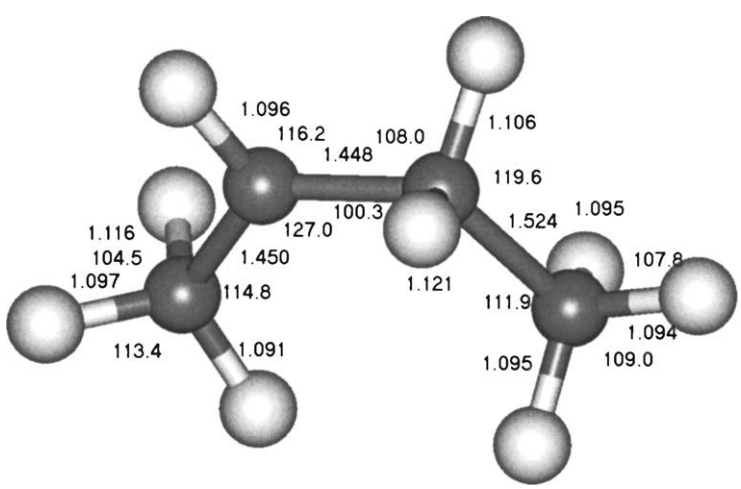

Fig. 6. Optimized structure for the classical *cis*-2-butyl ion obtained by QCISD/6-31G* theory.

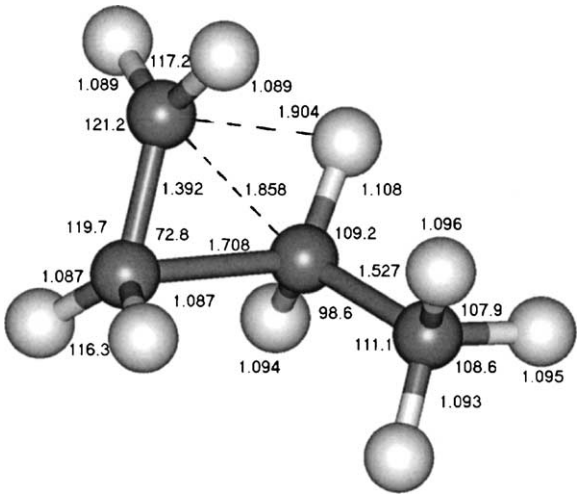

Fig. 7. Optimized structure for protonated methylcyclopropane obtained by QCISD/6-31G* theory.

experimental appearance energy [19]. The transition state for this pathway is given in Fig. 8. This is the lower energy pathway for methane elimination from $C_4H_9^+$ (Table 1). This and the CAD spectrum of the $C_3H_5^+$ product establish this pathway as the one operating at near threshold energies. As already noted, based on B3LYP/6-31G* intrinsic reaction coordinate (IRC) calculations, in this reaction an H from C2 migrates close to the central carbon and then goes on to form methane by insertion into the C1–C3 bond. Upon its closest approach to C1, the itinerant H is 1.1299 Å from that carbon, close to all of the other C–H distances of 1.09 Å in that structure. At this point the transferring H is 1.7564 Å from C1, and the breaking C2–C3 bond is extended to 1.7555 Å, so H-transfer and bond breaking are synchronous, as might be expected in what is essentially a displacement reaction. At the transition state, the itinerant H is only 1.1510 Å from C3, so methane is almost fully formed. Here, the C1–C3 distance is 2.5921 Å, so the system is passing through a $[CH_3C^+{=}CH_2\ CH_4]$ complex.

Two transition states were found in the pathway to 1,1-elimination from methylcyclopropane protonated on C2, the first at 235 kJ mol^{-1} (248.1 by B3LYP/6-31G* + ZPE theory) and the second at 246.7 kJ mol^{-1} (B3LYP/6-31G* + ZPE) above $\Delta_f H$(*tert*-$C_4H_9^+$). The earlier transition state also interchanges the two hydrogens at C1 of the protonated methylcyclopropane. IRC tracing [30,31] led from the earlier of these transition states to the later one and

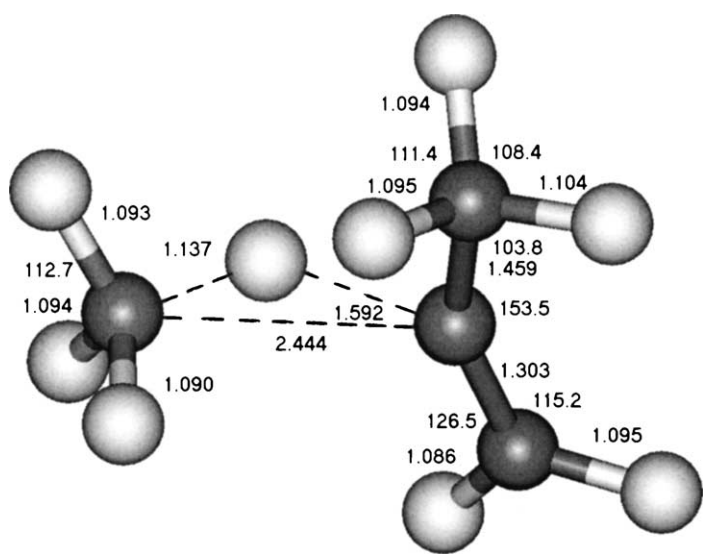

Fig. 8. Optimized structure obtained by QCISD/6-31G* theory for the transition state for methane elimination from $C_4H_9^+$ through an isobutyl cation-like stage.

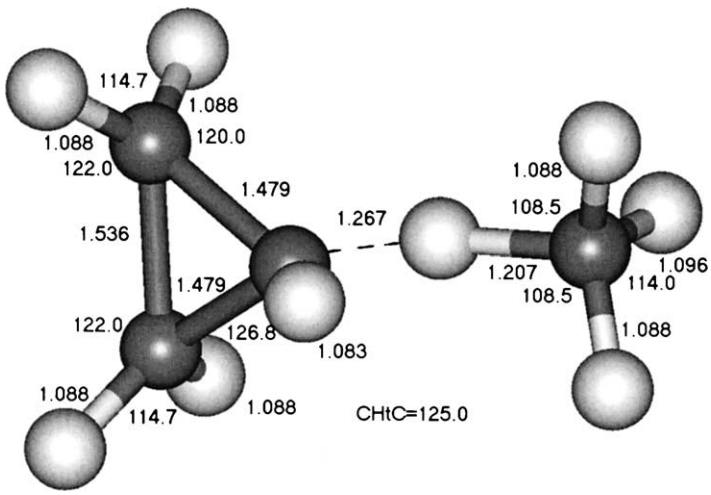

Fig. 9. Optimized structure obtained by QCISD/6-31G* theory for the transition state for methane elimination from protonated methylcyclopropane.

then through ring opening to $CH_2CHCH_2^+ + CH_4$ (Fig. 3), placing both transition states on the path to methane elimination. In the following, distances not in parentheses are for the earlier transition state according to QCISD/6-31G* theory (Fig. 9), and ones in parentheses were obtained for the later transition state by B3LYP/6-31G* theory because the later transition state was not located in QCISD theory, despite attempts to do so. In the two transition states that we located in the pathway to CH_4 elimination from protonated methylcyclopropane, the breaking C–C bond is stretched to 2.194 Å (2.534 Å) from 1.527 Å in protonated methylcyclopropane. At the second transition state the H is largely transferred and the C–C bond is largely broken. The transferring H is 1.267 Å (1.426 Å) from C2 and 1.207 Å (1.179 Å) from C3. Thus, in the earlier transition state, the migrating H is bonded to C1 and C3 to a similar degree, i.e., it is inserting into the C1–C3 bond. The migrating hydrogen is transferred from the methyl-bearing carbon to the methyl, making this a 1,1-elimination. The three-membered ring is quite intact at the first transition state as the length of the C3–C4 bond that is breaking is 1.536 Å, but that bond is starting to stretch (1.645 Å) at the second transition state. The transition states, although obtained without symmetry constraint, nonetheless both have a plane of symmetry containing the transferring H, the methyl carbon, the carbon that bears it, and the hydrogen attached to the last carbon.

Both pathways for methane elimination involve pentavalent carbons, i.e, nonclassical structures. Methane elimination from $CH_3CH{=}OH^+$ also has a transition state involving a pentavalent carbon [14], and a pentavalent stage occurs during methyl insertion into a C–H bond on the way to methane elimination from $CH_3CH_2CH{=}CH_2^{\bullet+}$ [7]. Dissociations of protonated alkanes are well-established examples of dissociations through pentavalent intermediates [32], so such species are involved in a variety of ionic dissociations.

The most probable translational energy release of about 10 kJ mol^{-1} [19] suggests that a substantial fraction of the metastable ions dissociate at energies significantly above threshold, given that the reaction takes place at its thermochemical threshold according to both appearance energy measurements [19] and the highest level of theory applied (compare the transition state energy and energy of the products in Table 1).

Table 2
Energies from theory for stationary points on the $C_3H_7^+$ potential surface

Structure	ZPE	B3LYP/6-31G*	QCISD/6-31G*	QCISD(T)/6-311G**
$CH_3CH^+CH_3$	228.4	−118.211835 (0)	−117.791477 (0)	−117.894759 (0)
$(CH_2\overline{CH_2CH_2})H^+$	236.3	−118.195414 (51.0)	−117.778096 (43.0)	−117.885405 (32.5)
H_2	26.1	−1.175482	−1.151698	−1.168336
$CH_2CHCH_2^+ + H_2$[a]	203.0	−118.147701 (143.0)	−117.730852 (133.8)	−117.834459 (132.9)
TS (c-$C_3H_7^+ - H_2$)	212.0	−118.101585 (273.1)	−117.668475 (271.2)	−117.790827 (256.5)
TS($CH_3CH_2CH_2^+ - H_2$)	219.2	−118.124424 (220.3)	−117.705288 (217.1)	−117.820286 (186.3)
TS(2-Pr → Int 1)	218.6[b]		−117.705457 (216.0)	−117.822338 (180.3)
Intermediate 1			−117.706188	−117.822443
Intermediate 2	223.6[b]		−117.706728 (217.7)	−117.822615 (184.6)
TS (− CH_4)	212.2	−118.044607 (422.9)	−117.619602 (435.1)	−117.735400 (402.2)

[a] The allyl value is from Table 1.
[b] Found at the MP2(fc)/6-31G* level because this structure was not found by B3LYP/6-31G* theory.

4. H_2 elimination from $C_3H_7^+$

Elimination of H_2 from $C_3H_7^+$ was studied to enable its comparison to the CH_4 eliminations from $C_4H_9^+$. Substantial improvements have occurred in theory since the previous characterizations of the dissociations of $C_3H_7^+$ [27,33], making it ripe for reinvestigation. As in $C_4H_9^+$, two pathways were found for H_2 elimination from $C_3H_7^+$, one by passage through a structure close to that of the 1-propyl cation and one from protonated cyclopropane; both produce the allyl ion. Energies of stationary points are given in Table 2, the structure of protonated cyclopropane in Fig. 10 and the structures of transition states located in Figs. 11 and 12. The transition state from protonated cyclopropane was found in 1976 by Schwarz and coworkers using semi-empirical theory [27]. The transition states we located also correspond to ones found by ab initio theory by Uggerud and coworkers [25,33]. Those investigators found elimination through 1-propyl cation to be the lower energy pathway, a conclusion that our results support. Thus, that is probably the major pathway for H_2 elimination from $C_3H_7^+$.

IRC tracing with B3LYP/6-31G* theory demonstrated that elimination starting from the 2-propyl cation involves isomerization of that ion through a 1-propyl-like configuration and then through a pentavalent stage to a transition state in which the departing H_2 is nearly fully formed (Figs. 11 and 13). Elimination takes place by union of the itinerant hydrogen with one on the remaining methyl, making this reaction a 1,1-like elimination. The latter part of the reaction coordinate is more complex under QCISD/6-31G* theory—with that theory we located a transition state between 1-propyl and an energy minimum, two energy minima and a transition state between the second energy minimum and $C_3H_5^+ + H_2$. Presumably, more effort would have located a third transition state between the two minima. All of these

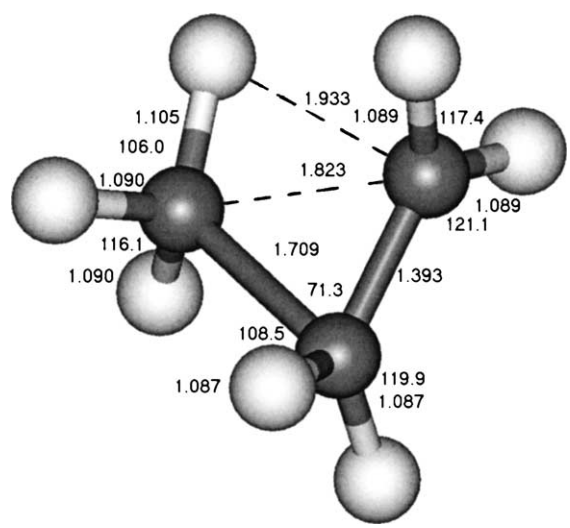

Fig. 10. Optimized geometry of protonated cyclopropane obtained by QCISD/6-31G* theory.

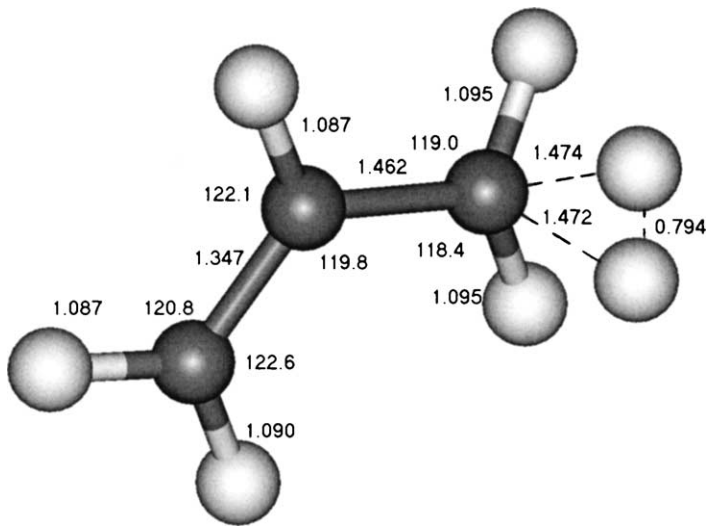

Fig. 11. Optimized geometry of the transition state obtained by QCISD/6-31G* theory for H_2 elimination through a 1-propyl-like stage.

points occur during the departure of H_2, which starts with its bond parallel to the C2–C3 bond and rotates to being perpendicular to that bond during separation of the products. All of the stationary points between the first transition state and the dissociated products have very similar energies, so they occur on a flat region of the potential surface, i.e., reflecting ion–neutral complex formation since the H_2 is essentially fully formed in this region. The hydrogens of H_2 are almost equidistant from C3 in the first QCISD transition state (1.1836 and 1.2013 Å), and much closer to C3 than to C2 (1.6930 and 2.4366 Å from C2).

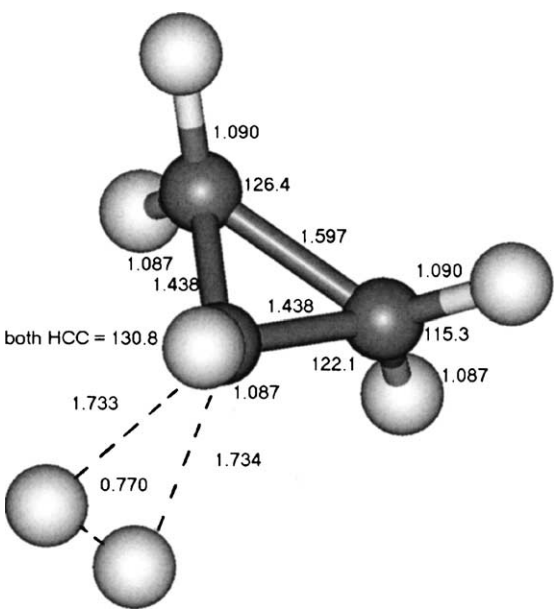

Fig. 12. Optimized geometry of the transition state for H_2 elimination from protonated cyclopropane obtained by QCISD/6-31G* theory.

Our most sophisticated level of theory placed the transition state for H_2 elimination from protonated cyclopropane (Fig. 12) 256 kJ mol^{-1} above the heat of formation of the 2-propyl cation. In the transition state for 1,1-H_2 elimination from protonated cyclopropane, the bridging hydrogen combines with an H from an adjacent carbon (Fig. 14), thereby avoiding a Woodward–Hoffmann barrier to direct 1,2-elimination. In the earlier transition state located by QCISD theory, the C–H distances to both departing H's in the incipient H_2 are the same length, clearly making this a 1,1-elimination. IRC tracing demonstrated that the ring opens to $CH_2CHCH_2^+$ in this reaction, paralleling CH_4 elimination from protonated methylcyclopropane.

A transition state was also found for dissociation of *sec*-$C_3H_7^+$ to $CH_3C^+ + CH_4$ at 402 kJ mol^{-1} above $\Delta_f H$(*sec*-$C_3H_7^+$) (QCISD(T)6-311G** theory). This

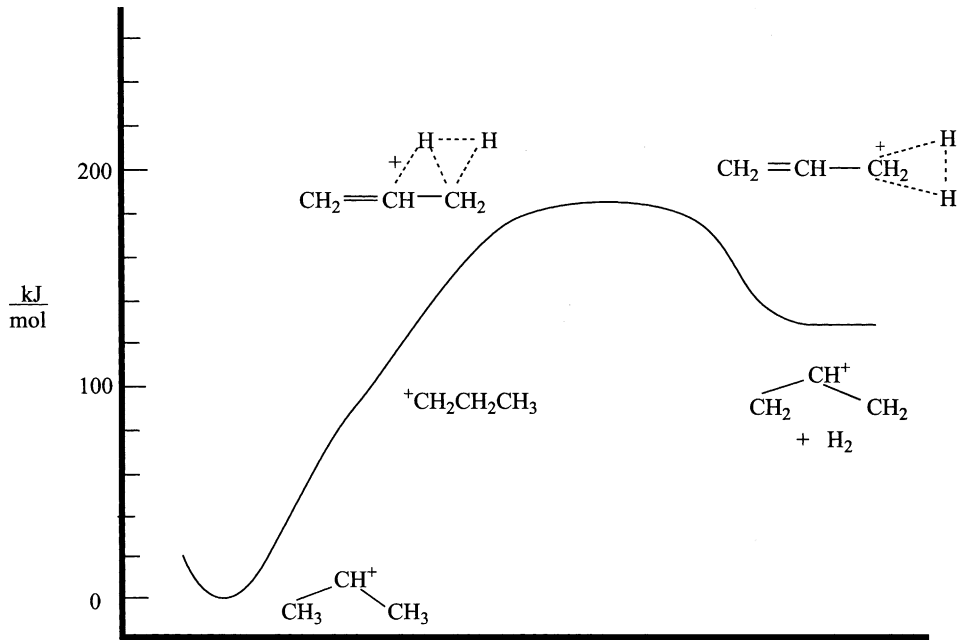

Fig. 13. Potential energy diagram for H_2 elimination from $C_3H_7^+$ through a 1-propyl-like stage.

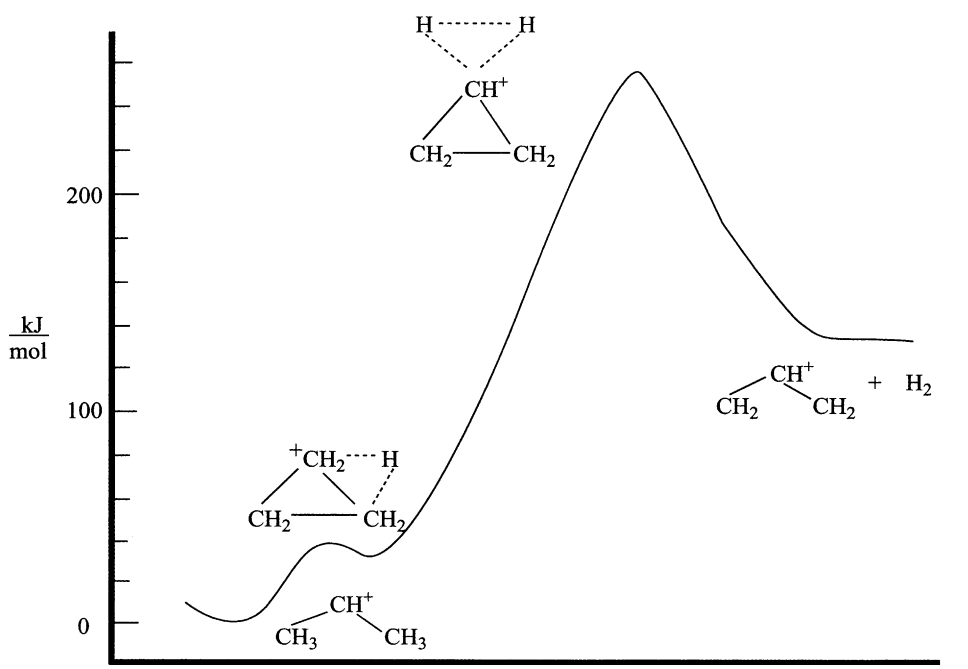

Fig. 14. Potential energy diagram for H_2 elimination from $C_3H_7^+$ through protonated cyclopropane.

transition state is much too high in energy for reaction through it to be significant.

5. Summary

Methane elimination from $C_4H_9^+$ and H_2 elimination from $C_3H_7^+$ both occur essentially by 1,1-eliminations. In both systems, a lower energy pathway to elimination goes through a primary carbocation-like structure, but a parallel higher energy pathway through protonated methylcyclopropane or protonated cyclopropane to the elimination products also exists in each case. Concerted 1,2-transition states are commonly bypassed in dissociations of ions in the gas phase by simple cleavages to form ion–neutral complexes followed by H-transfers to complete the elimination [1,6]; this type of mechanism is not indicated in the present study. Thus, the concerted transition states for CH_4 elimination from $C_4H_9^+$ and H_2 elimination from $C_3H_7^+$ provide an additional type of pathway around the high Woodward–Hoffmann barriers to synchronous concerted 1,2-eliminations [23,25]. Pentavalent structures occur in all characterized pathways, so hypervalent structures akin to protonated alkanes can be intermediates or transition states in reactions of ions in the gas phase. Present and other 1,2-H_2 eliminations from cations involve distortions that bypass the associated Woodward–Hoffmann barriers [25]. Furthermore, transition states for isomerizations involving forbidden 1,3-H-transfers are distorted in cations [34–36], radical cations [37], and anions [36] such that the associated reactions also circumvent symmetry imposed barriers, demonstrating a general circumvention of Woodward–Hoffmann barriers in ion chemistry. This is consistent with the statement of Woodward and Hoffmann regarding their rules “Violations There are none!” [21].

References

[1] D.J. McAdoo, Mass Spectrom. Rev. 7 (1988) 363.
[2] D.J. McAdoo, J.C. Traeger, C.E. Hudson, L.L. Griffin, J. Phys. Chem. 92 (1988) 1524.
[3] J.C. Traeger, C.E. Hudson, D.J. McAdoo, J. Phys. Chem. 92 (1988) 1519.
[4] S. Olivella, A. Solé, D.J. McAdoo, L.L. Griffin, J. Am. Chem. Soc. 116 (1994) 11078.
[5] S. Olivella, A. Solé, D.J. McAdoo, J. Am. Chem. Soc. 118 (1996) 9368.
[6] D.J. McAdoo, R.D. Bowen, Eur. Mass Spectrom. 5 (1999) 389.
[7] C.E. Hudson, D.J. McAdoo, Int. J. Mass Spectrom. 214 (2002) 315.
[8] D. Wang, R.R. Squires, D. Fărcasiu, Int. J. Mass Spectrom. Ion Processes 107 (1991) R7.
[9] D. Kuck, C. Matthias, J. Am. Chem. Soc. 114 (1992) 1901.
[10] D. Berthomieu, V. Brenner, G. Ohanessian, J.P. Denhez, P. Millié, H.E. Audier, J. Am. Chem. Soc. 115 (1993) 2505.
[11] H.E. Audier, G. Bouchoux, T.B. McMahon, A. Milliet, T. Vulpius, Org. Mass Spectrom. 29 (1994) 176.
[12] S. Beranová, C. Wesdemiotis, Int. J. Mass Spectrom. Ion Processes 134 (1994) 83.
[13] D. Berthomieu, V. Brenner, G. Ohanessian, J.P. Denhez, P. Millié, H.E. Audier, J. Phys. Chem. 99 (1995) 712.
[14] C.E. Hudson, L. DeLeon, D. Van Alstyne, D.J. McAdoo, J. Am. Soc. Mass Spectrom. 5 (1994) 1102.
[15] B. Davis, D.H. Williams, A.N.H. Yeo, J. Chem. Soc. (B) Phys. Org. (1970) 81.
[16] J.L. Holmes, A.D. Osborne, G.M. Weese, Org. Mass Spectrom. 10 (1975) 867.
[17] A. Maquestiau, R. Flammang, P. Meyrant, Int. J. Mass Spectrom. Ion Phys. 44 (1982) 267.
[18] M.C. Oliveira, T. Baer, S. Olesik, M.A. Almoster Ferreira, Int. J. Mass Spectrom. Ion Processes 82 (1988) 299.
[19] C. Aubry, J.L. Holmes, J. Phys. Chem. A 102 (1998) 6441.
[20] S.G. Lias, J.E. Bartmess, J.F. Liebman, J.L. Holmes, R.D. Levin, W.G. Mallard, J. Phys. Chem. Ref. Data 17 (1988) 68, 73, 114, 117.
[21] R.B. Woodward, R. Hoffmann, Angew. Chem. 8 (1969) 781.
[22] D.H. Williams, G. Hvistendahl, J. Am. Chem. Soc. 96 (1974) 6753.
[23] M.J.S. Dewar, H.S. Rzepa, J. Am. Chem. Soc. 99 (1977) 74.
[24] P.C. Burgers, J.L. Holmes, A.A. Mommers, J.E. Szulejko, Org. Mass Spectrom. 18 (1983) 596.
[25] E. Uggerud, Mass Spectrom. Rev. 18 (1999) 285.
[26] S. Sieber, P. Buzek, P.v.R. Schleyer, W. Koch, J. Walkimar de M. Carneiro, M. Carneiro, J. Am. Chem. Soc. 115 (1993) 259.
[27] H. Schwarz, W. Franke, J. Chandrasekhar, P. von Schleyer, Tetrahedron 35 (1976) 1969.
[28] M.J. Frisch, G.W. Trucks, H.B. Schlegel, G.E. Scuseria, M.A. Robb, J.R. Cheeseman, V.G., Zakrzewski, J.A. Montgomery Jr., R.E. Stratmann, J.C. Burant, S. Dapprich, J.M. Millam, A.D. Daniels, K.N. Kudin, M.C. Strain, O. Farkus, J. Tomasi, V. Barone, M. Cossi, R. Cammi, B. Mennucci, C. Pomelli, C. Adamo, S. Clifford, J. Ochterski, G.A. Petersson, P.Y. Ayala, Q. Cui, K. Morokuma, D.K. Malick, A.D. Rabuck, K. Raghavachari, J.B. Foresman, J. Cioslowski, J.V. Ortiz, A.G. Baboul, B.B. Stefanov, G. Liu, A. Liashenko, P. Piskorz, I. Komaromi, R. Gomperts, R.L. Martin, D.J. Fox,

T. Keith, M.A. Al-Laham, C.Y. Peng, A. Nanayakkara, M. Challacombe, P.M.W. Gill, B. Johnson, W. Chen, M.W. Wong, J.L. Andres, C. Gonzalez, M. Head-Gordon, E.S. Replogle, J.A. Pople, Gaussian, Inc., Pittsburgh, PA, 1998.
[29] A.P. Scott, L. Radom, J. Phys. Chem. 100 (1996) 16502.
[30] C. Gonzalez, H.B. Schlegel, J. Chem. Phys. 90 (1989) 2154.
[31] C. Gonzalez, H.B. Schlegel, J. Phys. Chem. 94 (1990) 5523.
[32] M. Alcami, O. Mó, M. Yanez, Mass Spectrom. Rev. 20 (2001) 195.
[33] J. Almlöf, G. Hvistendahl, E. Uggerud, Chem. Phys. 90 (1984) 55.
[34] C.E. Hudson, D.J. McAdoo, J. Am. Soc. Mass Spectrom. 9 (1998) 130.
[35] C.E. Hudson, D.J. McAdoo, J. Am. Soc. Mass Spectrom. 9 (1998) 138.
[36] C.E. Hudson, D.J. McAdoo, J. Org. Chem. 68 (2003) 2735.
[37] C.E. Hudson, D.J. McAdoo, Int. J. Mass Spectrom. 219 (2002) 295.